JOURNAL OF PROPULSION AND POWER
Vol. 21, No. 4, July–August 2005

Characterization of Pintle Engine Performance for Nontoxic Hypergolic Bipropellants

B. L. Austin*
IN Space LLC, West Lafayette, Indiana 47906
and
S. D. Heister† and W. E. Anderson‡
Purdue University, West Lafayette, Indiana 47906

Using rocket-grade hydrogen peroxide and a nontoxic, hypergolic miscible fuel, a 150-lbf thrust class pintle injector engine has been developed and tested with the aim of characterizing injector performance under a variety of design and operating conditions. Rapid, reproducible ignition was sustained under a wide range of operating conditions using the new hypergolic propellant combination. Parametric studies were undertaken to assess the influence of characteristic chamber length L^*, chamber diameter-to-pintle diameter ratio, total momentum ratio, secondary-to-primary hole diameter ratio, and the pintle length-to-pintle diameter ratio. High performance has been achieved in both steady-state and pulse mode operation.

Nomenclature

c^*	=	characteristic velocity
D_{pri}	=	primary hole diameter
D_{sec}	=	secondary hole diameter
I_{sp}	=	specific impulse
$I_{\text{sp}v}$	=	vacuum specific impulse
L^*	=	characteristic length
Pc	=	chamber pressure
$\rho I_{\text{sp}v}$	=	vacuum density specific impulse
$\in$	=	nozzle area ratio

Introduction

THE current standard in high-performing, storable bipropellants is the combination of nitrogen tetroxide (NTO) and monomethyl hydrazine (MMH). In addition to delivering high levels of specific impulse I_{SP}, the propellants are hypergolic, which greatly simplifies engine design and operation. However, both NTO and the hydrazine-based fuels (hydrazine, MMH, unsymmetrical dimethyl hydrazine, aerozine-50) pose significant health hazards. NTO has an exposure limit of 5 ppm, but a very high vapor pressure of 720 mmHg (Ref. 1). MMH, a carcinogenic liquid, has a relatively low vapor pressure of 36 mmHg, but a personal exposure limit of 200 ppb (Ref. 1). Here, exposure limit is defined as the time-weighted average that a person can be exposed to for a 40-h work week without deleterious health effects. Material safety data sheets specify the use of respirators in addition to full-body acid/chemical impermeable protection when handling these propellants. Furthermore, NTO requires rinse showering after handling. Given these handling requirements, as well as the extensive equipment, monitoring, and regulation necessary to ensure safe storage and use of the propellants, considerable effort has recently been put forth in investigating low or nontoxic alternative propellants with high performance.

Presented as Paper 2002-4029 at the AIAA 38th Joint Propulsion Conference and Exhibit, Indianapolis, IN, 7–10 July 2002; received 31 January 2004; revision received 22 December 2004; accepted for publication 24 December 2004.

*General Manager, 1220 Potter Drive, Suite 100. Member AIAA.
†Professor, School of Aeronautics and Astronautics, 315 North Grant Street. Associate Fellow AIAA.
‡Assistant Professor, School of Aeronautics and Astronautics, 315 North Grant Street. Member AIAA.

In 1993, the U.S. Naval Air Warfare Center Weapons Division (NAWCWD) at China Lake began searching for nontoxic propellants for use in divert and attitude control engines on ship-based ballistic missile defense intercept missiles.[2] By 1997, NAWCWD researchers had developed a class of storable, nontoxic fuels that were hypergolic with and completely miscible in rocket-grade hydrogen peroxide. The first of these nontoxic hypergolic miscible fuels (NHMFs), block 0, is a colloidal suspension of manganese oxide (Mn_3O_4) in methanol that approaches 93% of the vacuum specific impulse $I_{\text{sp}v}$ and 99% of the vacuum density specific impulse $\rho I_{\text{sp}v}$ of NTO/MMH when used with 98% hydrogen peroxide. Theoretical performance data of these two sets of bipropellants are shown in Fig. 1. When the NHMF fuels are used, the optimal performance occurs at mixture ratios near 2.75. This higher mixture ratio operation (as compared to NTO/MMH) is advantageous in that the bulk density is increased with the greater proportion of the denser oxidizer. The monopropellant characteristics of hydrogen peroxide also offer unique cycle advantages in that the fluid can be decomposed to run alternate power sources such as turbines, etc.

Prior efforts have focused on ignition delay determination of the RGHP/NHMF propellants and variants thereof.[3–7] This property is of significant interest because it directly impacts the ignitability of the mixture and the potential for "hard starts" due to excessive propellant pooling before ignition. The ignition delay of RGHP/NHMF is approximately 15 ms, which is substantially greater than the 2-ms ignition delay of NTO/MMH using the same drop tester.[5] The high vapor pressure of NTO is believed to provide a distinct advantage in this regard because vaporization is often proposed as a rate limiting step in these reactions.

To further the use of the RGHP and NHMF propellants in space and missile propulsion applications, experimental determination of engine parameters leading to high performance have been investigated in the current research. A pintle injector was selected for the workhorse engine based on its relative ease of manufacturing, inherent stability, and to support parallel efforts undertaken at other facilities.[8] The pintle injector design concept was initially developed as a standardized technique to test hypergolicity of storable propellant combinations under development in the late 1950s and is ideally suited for hypergolic propellants.[9] The concept requires machining of a single injector element, regardless of thrust level, and has a long history of use in hypergolic engines. TRW, Inc. (now a division of Northrop Grumman Corporation), pioneered developments of the injector concept; in Refs. 9–11 historical developments of the concept are detailed, with more recent applications detailed in Refs. 12–15.

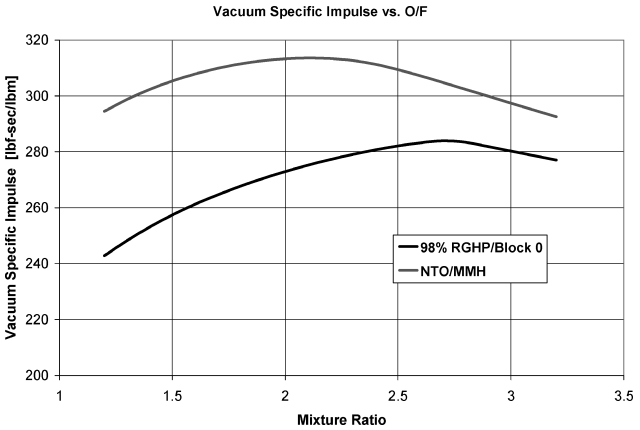

Fig. 1 Performance comparison of NTO/MMH and RGHP/NHMF propellants ($P_C = 500$ psia and $\epsilon = 10$).

The goal of the present work is to verify stable ignition and high-efficiency combustion of the new nontoxic hypergolic propellants using the pintle injector engine as a testbed. The test apparatus is discussed hereafter, followed by a summary of experimental results and conclusions.

Test Apparatus

Engine

A 150-lbf vacuum thrust-class pintle engine with a nominal 400-psia chamber pressure was designed and fabricated. The engine was designed to be modular to allow changes to the various geometries affecting the parameters of interest without constructing time-consuming and costly new engines for each parameter. Additionally, if part of the engine sustained damage from over-pressurization or ablation, the component could be replaced without having to reconstruct large engine components. The baseline pintle engine is shown in Fig. 2.

Fuel passes through the center of the pintle injector fitting and continues straight into the pintle post extending through the annulus injector plate and into the chamber. The pintle post sprays the fuel radially into the chamber through holes located near the tip of the post. The RGHP flows into two ports passing through the pintle injector plate and is guided radially inward through two channels in between the fuel and oxidizer manifold plates. The oxidizer turns 90 deg toward the chamber when it reaches the post and passes through a small (nominally 0.022-in.) gap, creating a cylindrical liquid sheet, or annulus, that flows down the pintle post. The fuel and oxidizer flows intersect and begin mixing at the fuel exit orifices around the pintle post.

Because hypergolic propellants do not require an additional source of ignition, combustion initiates a short distance away from the post.

The pintles used in this study all utilized two rows of equally spaced, circular holes; a row of primary holes, larger and closer to the injector face, and a row of secondary holes, smaller and closer to the pintle tip. A secondary hole diameter D_{sec} of 0.0150 in. was chosen as a nominal value because this was the smallest hole size that the machining facility could reliably and quickly drill. The primary hole diameter D_{pri} was select to be 0.0228 in. in the baseline design. To reduce the number of design variables, only cases with equal number of secondary and primary holes were considered for this research. For a 0.375-in.-diam pintle, 16 primary/secondary hole pairs were used to achieve a blockage factor, the fraction of the pintle's exterior perimeter that is taken up by injector orifices as seen from the annulus injector, of 0.5. Pintles used in this study had hemispherical exterior and interior tips. The rounded exterior prevents the establishment of a high-temperature recirculation zone that has the potential to damage the injector. The hemispherical interior was used to allow the fuel flowing through the pintle to absorb the heat energy.

For the engine size selected, a fuel-center pintle was preferred over an oxidizer-centered pintle for several reasons. Previous engines using RGHP and NHMF propellants experienced a hard start when the oxidizer preceded the fuel into the chamber. With the planned injector design, the annulus injector required a larger fill volume; thus, flowing oxidizer through the annulus would result in a fuel lead. Additionally, injecting fuel through the annulus at the desired velocity required a 0.0033-in. gap between the pintle and annulus wall. Given the ±0.0005-in. machining tolerances available, the variance in the fuel injection velocity could be upward of 30%. With the oxidizer having a mass flow rate almost three times that of the fuel, the machining tolerances were much less significant. Finally, for high fuel velocities, it was hypothesized that the fuel jets would penetrate the oxidizer annulus, resulting in a cooler, fuel-rich region near the chamber wall.

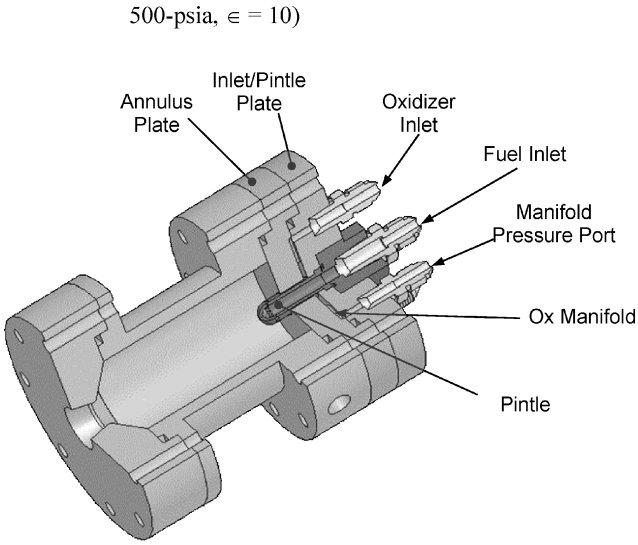

Fig. 2 Cutaway view of modular pintle engine.

The engine is composed of stainless-steel pintle and annulus injector/manifold plates, a copper chamber with a characteristic length of 29.6 in., and a copper nozzle plate. Stainless-steel pintles were used because copper and aluminum 6061-T6 pintles would either break or elongate at the primary row of holes under the pressure and heat loads. A combustion chamber wall thickness of 0.25 in. provided a safety factor of 1.25 over the yielding stress of the standard grade 2 bolts used to fasten the injector plates, chamber, and nozzle together. This allowed the chamber to separate from the injector plates or nozzle before the chamber wall breeching in the event of overpressurization. Table 1 is a summary of the relative pintle engine information.

Test Facility and Instrumentation

All pintle engine tests were conducted on the 1000-lbf test stand located in the Advanced Propellants and Combustion Laboratory within Purdue University's Maurice Zucrow Laboratories.[16] This facility utilizes a movable thrust flexure so that solid motors and hybrid, monopropellant, and bipropellant engines can be tested with minor adjustments. The test stand has a 4-gal hydrogen peroxide run tank as well as a 1-gal run tank for hydrocarbon fuels. Propellants are vacuum loaded into the run tanks, which can then be pressurized up to 1600 psia with gaseous nitrogen. Helium-pressurized, pneumatic ball valves are used for all propellant lines to provide fast response with minimal pressure loss.

The data acquisition system used during test fires is capable of recording 1000 sps at 16-bit resolution. Standard instrumentation at the rocket laboratory consists of a 1000-lbf interface load cell, 1000- and 3000-psia Druck pressure transducers, Omega k-type thermocouples, differential pressure transducers, and v-cone flow meters. In the present studies, cavitating venturies were used to limit the flow rates at startup, as well as to provide a means to calculate the mass flow rate based on water calibrations; the differential pressure transducers across the v-cone flow meters could not survive the water hammer effect created by using cavitating venturies downstream

Table 1 Baseline engine design

Parameter	Value	Units
General		
Chamber pressure	400	psia
Vacuum thrust	149	lbf
Vacuum specific impulse	231	s
Characteristic velocity	5159	ft/s
Characteristic length	29.6	in.
Mass flow rates		
Total	0.643	lbm/s
Oxidizer	0.471	lbm/s
Fuel	0.172	lbm/s
Mixture ratio	2.74	
Pintle		
Pintle diameter	0.375	in.
Pintle length	0.450	in.
Primary hole diameter	0.0228	in.
Secondary hole diameter	0.0150	in.
Number of hole pairs	16	
Fuel exit area	0.00936	$in.^2$
Fuel injection velocity	47.1	ft/s
Annulus		
Injector face hole diameter	0.418	in.
Gap distance	0.022	in.
Oxidizer exit area	0.0268	$in.^2$
Oxidizer injection velocity	28.4	ft/s.
Chamber		
Chamber diameter	1.7460	in.
Chamber length	3.0015	in.
Nozzle		
Throat diameter	0.5690	in.
Throat area	0.254	$in.^2$
Contraction ratio	9.42	
Exit diameter	0.7625	in.
Exit area	0.457	$in.^2$
Expansion ratio	1.799	

of the main valves. Data acquisition and control are accomplished using the National Instruments Labview software package. A National Instruments SCXI module provides the hardware interface to the instrumentation and control devices.

Testing Results

Once the engine hardware was fabricated, water-flow tests were performed to provide visualization of the propellant flow, calibration of venturies, and for leak checking the test stand and engine plumbing. Following the water-flow tests, the RGHP and NHMF propellants were tested in the engine with the nozzle plate removed. These open chamber tests served to determine the propellant injection times and verify hypergolic ignition without risking an overpressurization, which could harm the engine or test stand.

Over 150 test firings were conducted to determine the sensitivity of ignition and performance to various design changes under both 3-s steady-state and pulsing mode conditions. The first full engine test failed due to an overpressurization/hard start resulting from the fuel reaching the chamber approximately 0.33 s before the oxidizer. The second full engine test also resulted in a hard start when a slight oxidizer lead was encountered. In both incidents, the engine failed at the intended point, the bolts holding the chamber onto the injectors. Engine damage was light, and repairs were completed within a few hours.

The pintle engine was successfully fired for a 3-s test after control system and plumbing upgrades were implemented to achieve a small fuel lead. After cooling for a couple of minutes, two more 3-s tests were conducted. Tank ullage pressures, injector pressures, mass flow rates, and engine thrust data were acquired on all tests. The chamber pressure transducer failed midway into the second test, and so no chamber information was available from the third test. Posttest inspection of the engine components, including the pintle and nozzle throat, revealed no signs of erosion or wear.

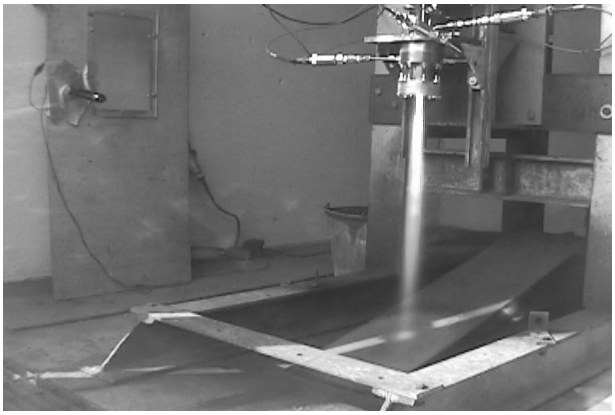

Fig. 3 Test fire of pintle engine on Purdue University's 1000-lbf test stand.

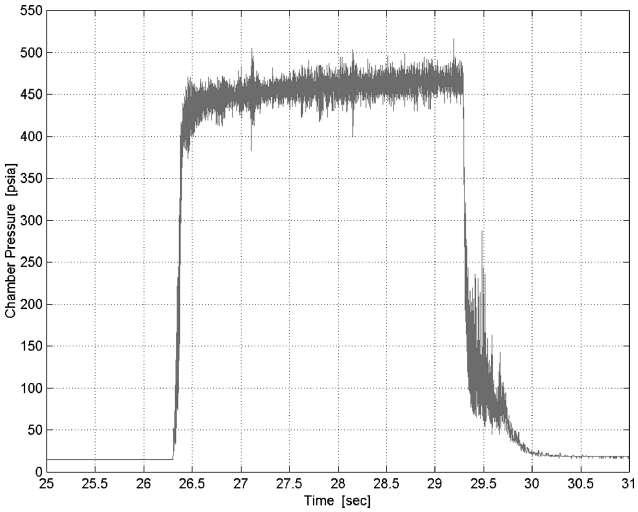

Fig. 4 Chamber pressure vs time for 3-s test.

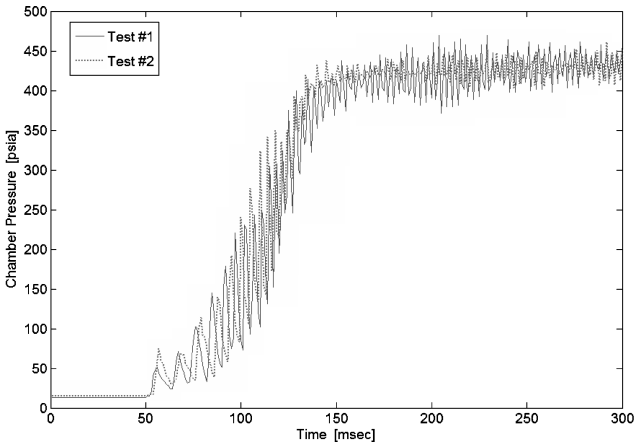

Fig. 5 Overlay of two unfiltered chamber pressure traces from two different test fires.

Since this initial success, the pintle engine has been successfully fired over 150 times in 3-s and pulsing tests. One of the test fires is shown in Fig. 3. Some of these tests were performed with varying mixture ratios of RGHP and block 0. The remainder of the test firings were conducted to examine pulse duty cycles and investigate the parametric design and injection conditions discussed hereafter.

Typical unfiltered chamber pressure data, like that in Fig. 4, has shown that there is no overshoot evident in the chamber pressure pointing to a smooth startup. An overlay of two chamber pressure traces, shown in Fig. 5, from two different test fires show that the pressures rise at the same rate to approximately the same point

with little or no overshoot. This indicates that the ignition process is smooth, repeatable, and reproducible. The chamber pressure reaches 90% of the steady-state level within 80 ms. With a bipropellant valve close coupled to the engine, it is believed that the startup time could be decreased to a fraction of that observed during the tests conducted for this study.

Usual variance in the chamber pressure signal is less than $\pm 10\%$ of the steady-state signal, indicating that the combustion is somewhat rough. A splash plate engine using the same propellants, mass flow rates, chamber, and nozzle has demonstrated a chamber pressure variation of only $\pm 4\%$ (Ref. 17). Despite taking considerable means to tighten the nut securing the pintle into the injector plate, the pintle post can be moved slightly toward the annulus wall by applying a moderate amount of pressure to the side of the pintle. Given this and the low noise in the splash plate engine (and many subsequent tests in other engine geometries), it is postulated that the combustion roughness in the pintle engine test is most likely the result of the pintle vibrating about the engine centerline due to pressure variations inside the chamber. This is an undesirable feature that results from the advantages of having modular components.

The fast Fourier transform of the chamber pressure data in Fig. 4 is shown in Fig. 6 (with the ordinate amplified 36 times) showing little organized activity between 0 and 500 Hz. The estimated L1 and T1 instability frequencies are orders of magnitude higher than the current 1000-sps data sampling rate can resolve. However, audible noise levels during the test fires did not indicate an instability.

The thrust data for the test shown in Fig. 4 are shown in Fig. 7. The thrust levels trace the chamber pressure and are also repeatable in terms of thrust level, rise times, and startup and shutdown transients. Further more, the variation in the thrust signal is about the same percentage as the variation in the chamber pressure.

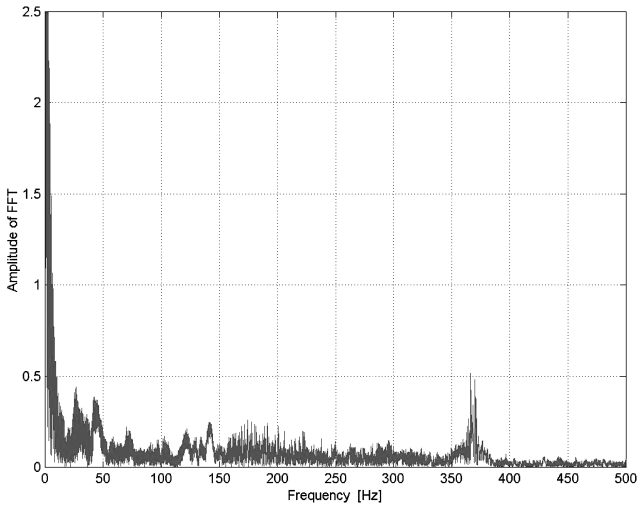

Fig. 6 Fast Fourier transform of chamber pressure (with scale amplified 36 times).

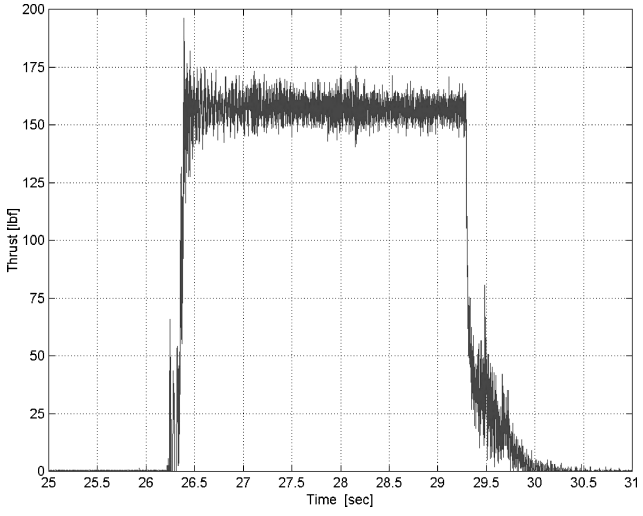

Fig. 7 Thrust vs time for 3-s test.

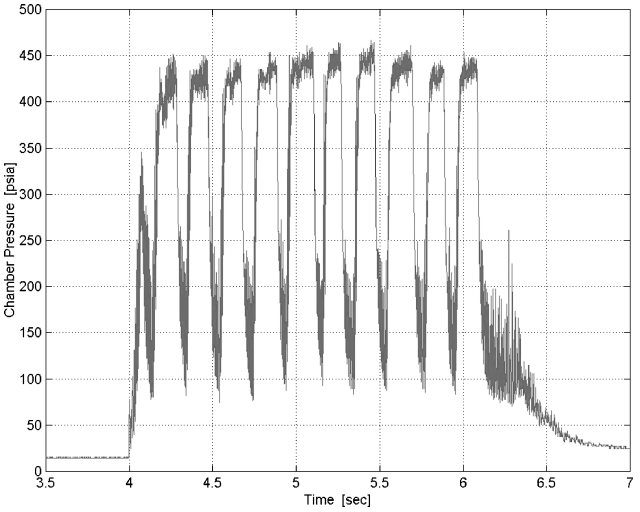

Fig. 8 Chamber pressure vs time for pulse test with 11 0.1-s on/0.1-s off cycles.

To provide a degree of accuracy in the measured data and calculated results, the error analysis methodology outlined by Cahill et al.[18] was employed. With a lack of pressure and force standards, end-to-end calibrations of the pressure transducers and load cell could not be performed. However, both of these devices were calibrated in place as a standard procedure before testing. Estimates for the bias error were made based on information supplied by the instrumentation manufacturers. Bias errors of 15 and 5 psi were reported for the Druck 3000- and 1000-psi devices, respectively, with a precision of 1.29 psi for both devices. The interface load cell had a bias limit of 2.651 lbf with a precision of 0.876 lbf. Oxidizer and fuel venturies had bias errors of 0.65 and 0.45%, respectively. With this methodology and these approximations, the errors in the c^* efficiency and specific impulse were estimated to be approximately $\pm 2.3\%$ and ± 5 s, respectively. Reference 19 provides a complete description of the error analysis.

Several pulsing operation tests were also conducted by using a 0.1-s pulse duration. To ensure that ignition would take place during the short duration, a single 0.1-s duration test was executed. Following that success, one 5-pulse and two 11-pulse tests were conducted. The chamber pressure trace of an 11-pulse test is shown in Fig. 8. The thrust signal clearly indicates 11 pulses with only the first one being significantly lower than the rest. The first pulse in the set is expected to be lower than the rest given that the feed lines are clear before that pulse and relatively full for all of the others. Whereas this testing demonstrated pulse-to-pulse repeatability, the valving and manifolding used in the facility are not optimal to test truly the minimum pulse widths achievable with this system.

An acrylic chamber was constructed and fired in an attempt to determine the startup transient and initial flow patterns. An image from the 6-s firing is shown in Fig. 9. Whereas the ignition event was not captured by the 60-fps camera, posttest analysis of the chamber interior showed that the wall receded uniformly by approximately 0.25 in. with the exception of 16 small locations (approximately 0.25 in. in diameter), which showed about a 0.08-in. recession, 0.48 in. aft of the injector face. This evidence, combined with the close-up video in Fig. 10 showing fuel impacting the chamber wall, verifies that, for a chamber diameter of 1.75 in. and a fuel injection velocity of 47.1 ft/s, the fuel exiting the primary pintle holes penetrates the oxidizer flow and cools the chamber wall directly opposite the injection locale.

Steady-State Parametric Test Results

Once testing reached the point of consistently and reliably providing data, parametric studies were initiated. Each parameter was tested in two 3-s firings resulting in a total of 60 steady-state tests.

Fig. 9 Test firing with acrylic chamber.

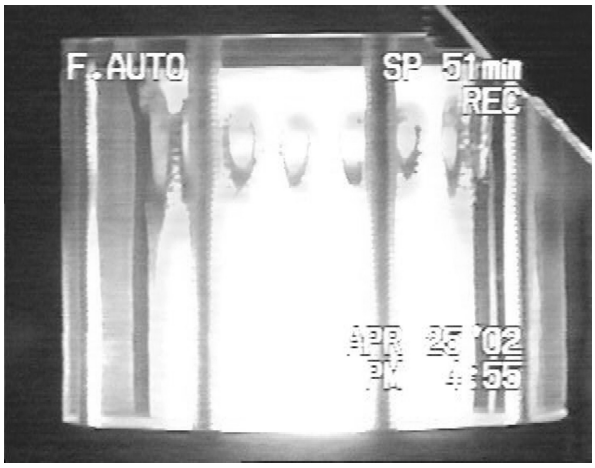

Fig. 10 Close-up of acrylic chamber showing radial fuel jet impact points on outer chamber wall.

The characteristic length and narrow- and wide-chamber total momentum ratio (TMR) tests were also tested in a total of 37 pulse tests. The following sections detail the results from the parametric tests. All c^* efficiencies are based on a one-dimensional, equilibrium, theoretical characteristic velocity of 5159 ft/s obtained assuming one-dimensional equilibrium thermochemistry. Many of the c^* efficiencies reported in the following parametric studies are at or above 100%, a problem attributed mainly to transducer drift due to heating during the firing.

Because the primary goal of the studies was focused on characterizing ignition performance, no snubbers were utilized in the passage from the transducer to the chamber. Whereas this approach provided high resolution of ignition transients, a substantial amount of upward drift was observed in the steady-state portion of the firing due to heating of the pressure transducer from chamber gases. As a result, transducers were subjected to temperatures as high as 300°F as measured with a shielded thermocouple during a typical test. Experiments conducted in heating a transducer to this level showed a drift of 10 psia that introduces a 2–3% bias into the c^* calculations throughout. Numerous other groups have encountered this problem when testing small engines; we presume that relative comparisons in the results are still valid in drawing conclusions about performance sensitivities to design changes.

In some cases, the measured specific impulses are above the theoretical maximum of 188 s predicted using equilibrium thermochemistry. Given the substantial difference between the measured and theoretical values, it is believed that the load cell measuring the engine thrust may have gone out of calibration. Because the main goal of the study was to identify sensitivities of performance to design changes, these error sources are viewed as biases that do not disturb the measured trends.

Characteristic Length Variations

Given the modular design of the engine, the characteristic length L^* was easily varied by using different combinations of three chamber sections. The c^* efficiency and specific impulse increased as the engine's characteristic length increased as shown in Fig. 11, indicating excellent combustion at L^* values of 30 in. or greater. The general trend agrees well with theory because increasing L^* increases the chamber residence time, therefore permitting the propellants more time to mix, evaporate, and combust. Whereas performance improved with L^* (and, thus, chamber volume) increasing by a factor of four; test data revealed no discernable effects on the chamber pressure rise time. This indicates a robust ignition using the RGHP/NHMF propellants in a pintle injector engine.

Chamber Diameter Variations

Because changing the pintle diameter would alter the angular spacing between the pintle holes as well as the annulus injector

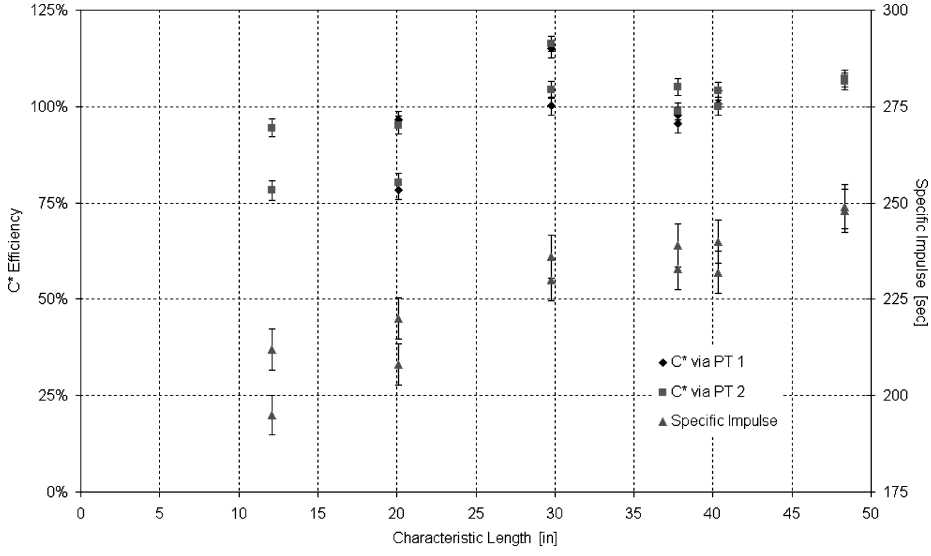

Fig. 11 Efficiency of c^* and I_{sp} vs characteristic length.

area, the chamber diameter was varied to change the chamber diameter to pintle diameter ratio. However, given the machining and testing time requirements, there was only enough time to test one chamber diameter to pintle diameter ratio beyond the baseline ratio. With the injector pattern and velocities, a wider chamber was more likely to result in higher combustion efficiency than a narrower one. The largest chamber diameter that could be used in the modular engine without risking damage to the O-rings was 2.25 in., thus, this size was constructed. When the chamber diameter was increased, the contraction ratio increased from the 9.5 of the baseline chamber to 15.6.

Because two points are an insufficient number on which to base a trend, no c^* efficiency or I_{sp} graphs for this test series are presented, though both test conditions are included in the TMR studies (narrow and wide chambers) at the baseline TMR of 0.61. When the data from these two tests are compared, the average c^* efficiency of the narrow chamber is 11.4% higher than that of the wide chamber. However, when the specific impulses are compared, the two tests are equivalent within the estimated error. Additional testing would be required to further quantify these differences.

TMR Variations

The TMR, defined as the momentum rate of the propellant flowing through the pintle divided by the momentum rate of the propellant flowing through the annulus, is one of the primary design parameters for pintle injectors. Given that changes in mass flow rates result in changes in chamber pressure or mixture ratio, the TMR study was performed by varying the fuel and oxidizer velocities while keeping the mass flow rates constant. Two additional pintles providing 24.1 and 66.7 ft/s fuel injection velocities and two additional oxidizer plates providing 17.7 and 23.7 ft/s oxidizer injection velocities were constructed. This permitted testing of nine different TMR combinations ranging from 0.30 to 1.36.

For the narrow chamber, the c^* efficiency and I_{sp} graphs shown in Fig. 12 have logarithmic shapes, which appear to asymptote at a TMR of approximately 0.7. When the lowest TMR for the narrow chamber was tested, the propellants initially ignited but were extinguished within 100 ms of the start of the chamber pressure rise. From the video, it appears that the peroxide continued to decompose, to an extent, for the remainder of the test. The c^* efficiencies and specific impulses reported at this lower TMR are the values obtained at the beginning of the tests because the chamber did not achieve steady-state operation.

Unlike the narrow chamber tests, the measured c^* efficiency and I_{sp} of the TMR study done with the wide chamber are relatively insensitive to the TMR as seen in Fig. 13. Additionally, there were no incidents of propellants extinguishing at even the lowest TMR conditions tested.

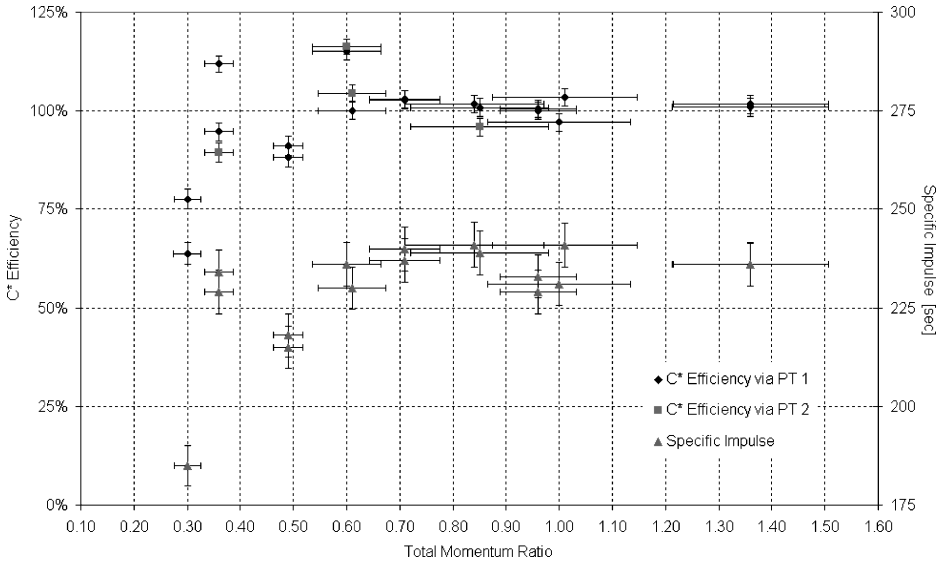

Fig. 12 Efficiency of c^* and I_{sp} vs TMR with 1.75 in.-diam chamber.

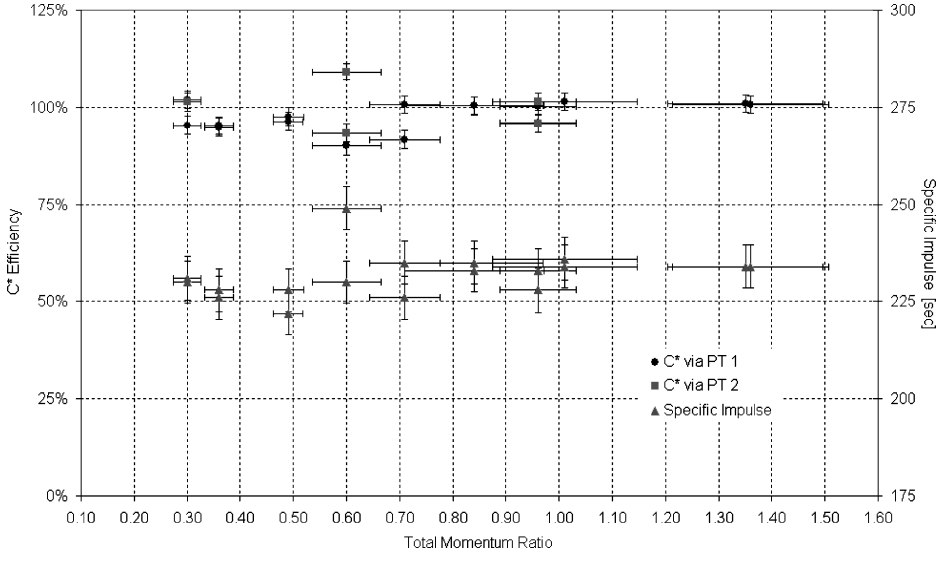

Fig. 13 Efficiency of c^* and I_{sp} vs TMR with 2.25-in.-diam chamber.

Secondary-to-Primary Orifice Diameter Ratio

In an effort to isolate the orifice diameter ratio study from the TMR, it was necessary to keep the fuel exit area as close as possible to the baseline case. However, this was limited by the drill bit sizes available from suppliers and the angular resolution of the equipment used to locate and drill the holes. The baseline secondary hole diameter of 0.0150 in. was selected for all of the ratios (except for the $D_{sec}/D_{pri} = 1.00$ case, where $D_{sec} = 0.0157$ in.). Primary orfice diameters were calculated for an incremental number of primary/secondary hole pairs using the baseline exit area. The primary hole diameter and number of hole pairs were then selected based on which ones resulted in a "convenient" angular spacing. Given these constraints, pintle posts were constructed with primary hole diameters of 0.0420, 0.0276, 0.0189, and 0.0157, resulting in 6, 12, 20, and 24 primary/secondary hole pairs, respectively.

As shown in Fig. 14, the c^* efficiency decreases slightly as the secondary to primary hole diameter ratio increases, and the I_{sp} does not vary significantly outside of the estimated error. In typical liquid-rocket engines, smaller injector orifices produce smaller propellant droplets that, in general, lead to better combustion efficiency given that the time required to evaporate a drop increases with the square of the drop diameter. Because the characteristic velocity and specific impulse do not increase as the primary hole diameters decrease, the diameter of the drops formed in pintle injector engines must be determined by another parameter or there must be adequate residence time to evaporate and combust these larger drops. Atomization and mixing may also be controlled or affected by radial fuel jet impingement on the walls of the chamber as indicated in Fig. 8 and 9.

Pintle Length Variations

The length of the pintle influences the wall heat transfer and the chamber residence time. Because the tests were of short duration and conducted with a heat sink chamber, the effect of the heat transfer could not be studied in detail. However, the chamber residence time was assessed in the short duration tests via measurement of c^* efficiency and I_{sp}. To optimize the flowfield created by the pintle, it is desirable to use a curved injector face. Manufacturing limitations did not permit this feature to be included in the testing in this program. For the same reasons mentioned in the chamber diameter to pintle diameter study, the pintle length was altered to vary the pintle length to pintle diameter ratio rather than changing the pintle diameter.

As seen in Fig. 15, c^* efficiency decreased by 5% and I_{sp} decreased by almost 11% when the pintle length was increased from 0.462 to 1.262 in. This decrease is likely the result of the longer pintles causing the propellant residence time to decrease and less propellant to combust inside the chamber. Also noted during this test series was that the noise in the chamber pressure signal increased from about

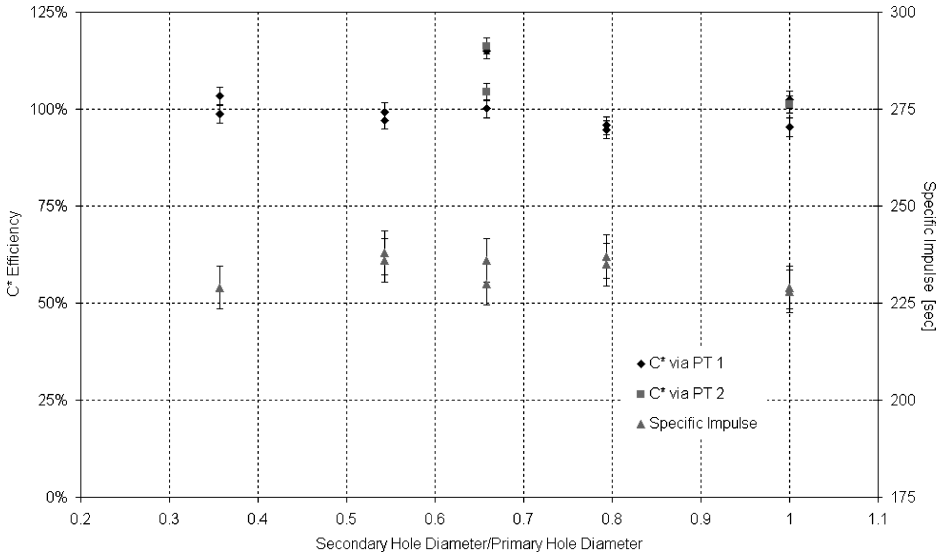

Fig. 14 Efficiency of c^* and I_{sp} vs secondary-to-primary hole diameter ratio.

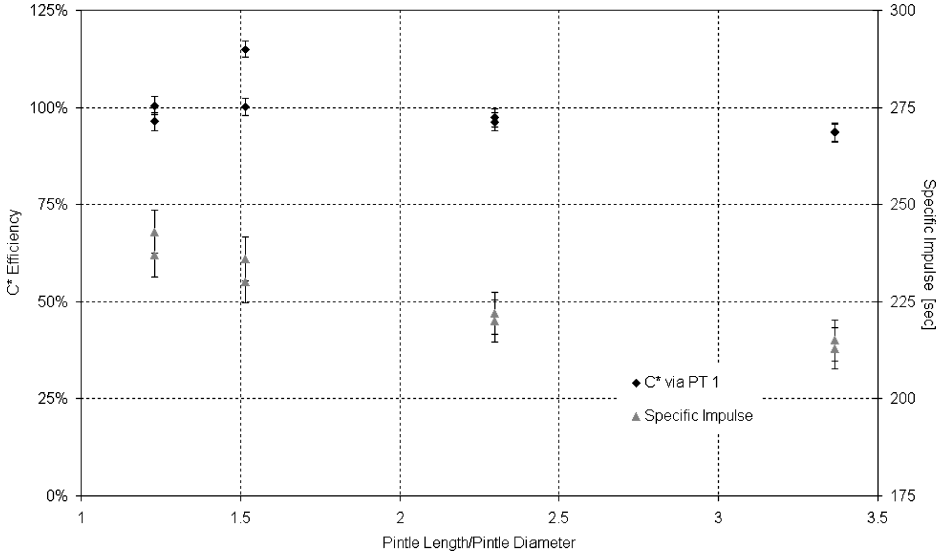

Fig. 15 Efficiency of c^* and I_{sp} vs pintle length-to-pintle diameter ratio.

12% of the steady-state signal to as much as 37% as the pintle length increased. This observation supports the speculation that the combustion roughness is the result of the pintle oscillating about the centerline of the engine.

Pulse Mode Parametric Test Results

Pulse tests were conducted for the characteristic length and TMR tests. These tests followed the 11 0.1-s on/0.1-s off cycles discussed earlier. The characteristic velocity efficiencies, specific impulses, and other statistical results presented are based on the last 10 of the 11 pulses because the lack of propellants in the feed lines leading up to the injector at the start of the pulse tests consistently lead to much lower performance of the first pulse than the remainder of the pulses.

The c^* efficiency and specific impulse of each 0.1-s pulse are shown in Fig. 16 for each characteristic length tested. As is evident in Figs. 16, the c^* efficiencies and specific impulses increase as L^* increases, the same trend observed in the 3-s burn duration tests. In this case, it appears there is a benefit in increasing L^* beyond 30 in. for optimal performance in a pulsing mode.

Unlike the logarithmic shape of the performance curves of the 3-s narrow chamber TMR tests, the c^* efficiency and I_{sp} of the narrow chamber TMR pulse tests are relatively flat, as seen in Fig. 17. That the lower TMR pulse tests have higher c^* efficiencies and specific impulses than their 3-s duration counterparts is believed to be the consequence of the hydrogen peroxide having insufficient time to "quench" the combustion as appeared to occur in the steady-state tests of this configuration, that is, there may have been insufficient combustion to vaporize and react all of the hydrogen peroxide under steady-state flow conditions. The c^* efficiency and I_{sp} of the TMR pulses tests with the wide chamber shown in Fig. 18 appear to be very similar to the steady-state performance.

A concern of pulse testing the pintle engine was that the engine be able to achieve repeatable and consistent chamber pressures. Whereas each pulse plotted in Figs. 16–18 displays the amount of variation in the c^* efficiencies and specific impulses of each test, the standard deviation in the chamber pressure for each pulse test was also determined. Most of the pulse tests had a standard deviation in the maximum chamber pressure of 15 psi or less, less than 4% of the mean chamber pressure.

Whereas the chamber pressure during the on portion of the pulse operation reach levels comparable to the steady-state testing, the chamber pressures did not return to atmospheric between pulses. This behavior is an artifact of the plumbing and valving configuration employed in the test facility and would be strongly influenced by the use of a bipropellant valve close coupled to the injector. The average chamber pressure during the off portion of pulse testing was approximately 85 psia with minimums of 38 psia and maximums of 153 psi. There was approximately twice as much variation in the

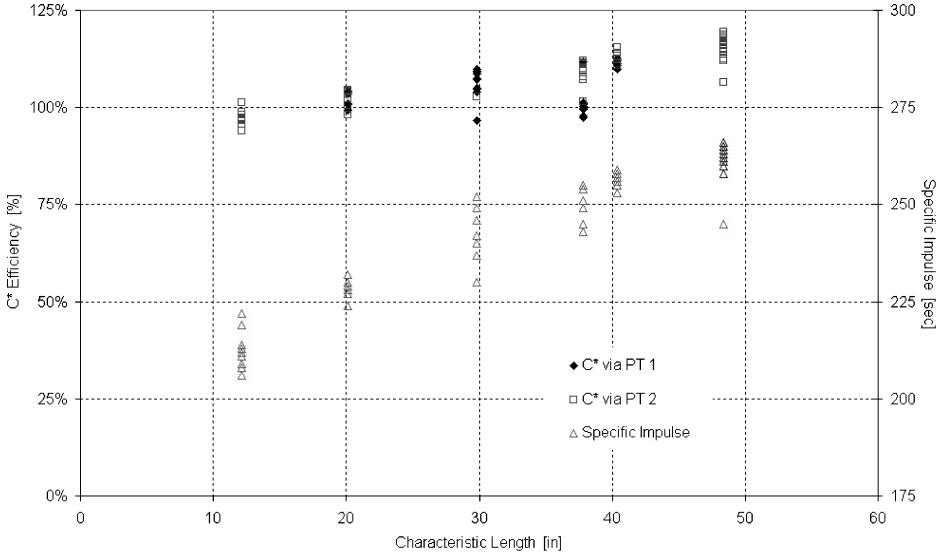

Fig. 16 Efficiency of c^* and I_{sp} vs characteristic velocity for pulse tests.

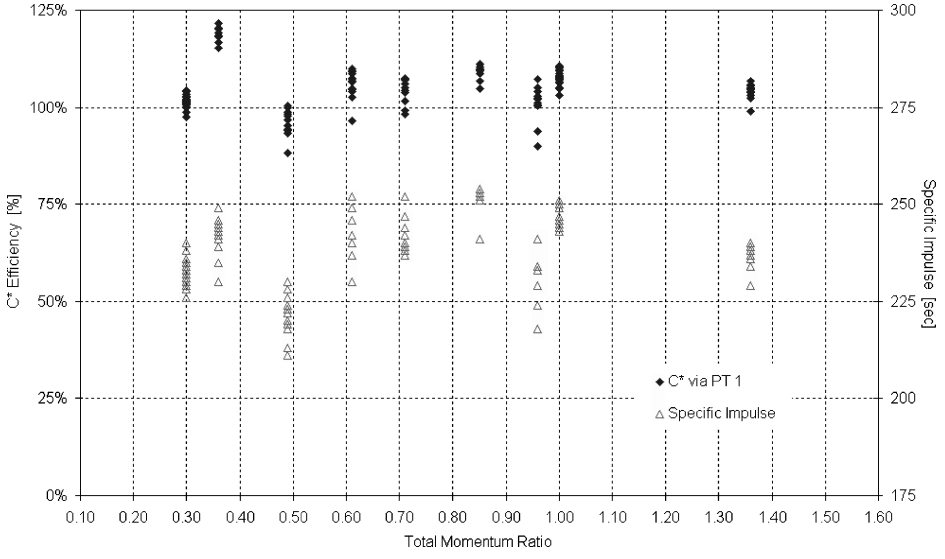

Fig. 17 Efficiency of c^* and I_{sp} vs TMR with ϕ1.75-in. chamber for pulse tests.

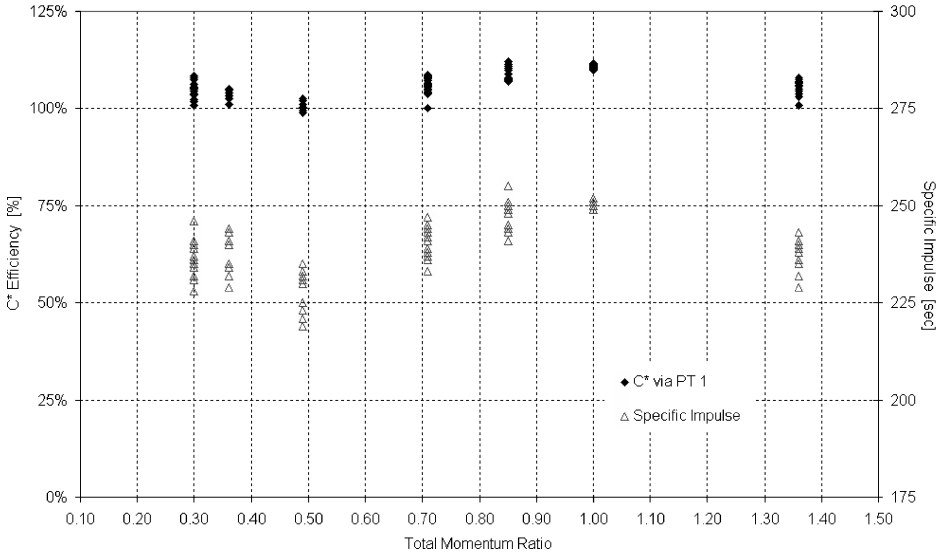

Fig. 18 Efficiency of c^* and I_{sp} vs TMR with ϕ2.25-in. chamber for pulse tests.

chamber pressure between pulses than there was in the chamber pressure during the pulses.

Conclusions

A modular pintle engine has been fabricated and successfully tested with nontoxic hypergolic bipropellants based on hydrogen peroxide and a methanol fuel laced with catalyst. Rapid, reproducible ignition has been demonstrated with this propellant combination under both single- and multiple-pulse firings. Typical rise times are on the order of 80 ms under both single- and multipulse conditions. Whereas the combustion is somewhat rough, no organized frequency content was discernable in the chamber pressure measurements. Combustion roughness levels of about 10% are attributed to the modular nature of the engine in that the pintle post is subject to some vibration.

Parametric studies were conducted to identify the influence of total momentum ratio L^*, chamber diameter, pintle hole sizes, and pintle length. Steady-state combustion was optimized for L^* values greater than 30 in. and TMR values greater than 0.7 for the baseline 1.75-in. diam chamber. Good performance was achieved over the 0.3–1.36 TMR range with the larger 2.25-in.-diam chamber. Performance was insensitive over the range of pintle hole sizes tested, and shorter pintles led to improved performance for the flat-face injector employed in these tests. The testing of a transparent 1.75-in.-diam chamber showed fuel spokes impinging on the chamber wall at nominal TMR conditions, a factor that explains the relative insensitivity of performance in this small engine.

Excellent performance under pulsing conditions was also demonstrated, although there is evidence that slightly larger L^* values would be required to optimize c^* for pulsed operation. There were no distinct effects of TMR on performance under pulsing conditions.

Acknowledgments

The authors would like to thank the late Ron Humble of KB Sciences and Martin Minthorn of the U.S. Naval Air Weapons Center (NAWC) China Lake, for funding the research efforts under a Phase 2 SBIR with the Ballistic Missile Defense Organization (now MDA) and NAWC. We also acknowledge the help of Senior Engineer Scott Meyer of Purdue University for his immense help in improving engine testing.

References

[1]"Chemical Sampling Information," URL: http://www.osha-slc.gov/dts/chemicalsampling/toc/toc_chemsamp.html.

[2]Meade, C. J., Lormand, B. M., and Purcell, N. L., "Status of Non-Toxic Hypergolic Miscible Fuel Development at NAWCWD China Lake" *2nd International Hydrogen Peroxide Propulsion Conference*, Nov. 1999.

[3]Palmer, R. K., "Development and Testing of Nontoxic, Hypergolic Miscible Fuels," M.S. Thesis, School of Aeronautics and Astronautics, Purdue Univ., West Lafayette, IN, 2001.

[4]Pourpoint, T. L., and Rusek. J. J., "Investigation of Homogeneous and Heterogeneous Catalysis for the Propulsive Decomposition of Hydrogen Peroxide," *International Conference on Green Propellant for Space Travel*, European Space Research and Technology Centre, Noordwijk, The Netherlands, June 2001.

[5]Frolik, S., "Hypergolic Liquid Fuels for Use with Rocket Grade Hydrogen Peroxide," M.S. Thesis, School of Aeronautics and Astronautics, Purdue Univ., West Lafayette, IN, 2001.

[6]Frolik, S., et al., "Development of Hypergolic Liquid Fuels for Use with Hydrogen Peroxide," AIAA Paper 2000-3684, July 2000.

[7]Funk, J. E., et al., "Development Testing of Non-Toxic, Storable, Hypergolic Liquid Propellants," AIAA Paper 99-2878, June 1999.

[8]Humble, R. W., "Liquid, Hypergolic, Bipropellant Engine System Development Using Methanol and Hydrogen Peroxide," *2nd International Peroxide Symposium*, 1999, pp. 289–298.

[9]Dressler, G. A., and Bauer, J. M., "TRW Pintle Engine Heritage and Performance Characteristics," AIAA Paper 2000-3871, July 2000.

[10]Elverum, G., Staudhammer, P., Miller, J., Hoffman, A., and Rockow, R., "The Descent Engine for the Lunar Module," AIAA Paper 67-521, July 1967.

[11]Gilroy, R., and Sackheim, R., "The Lunar Module Descent Engine—A Historical Perspective," AIAA Paper 89-2385, 1989.

[12]Fritz, D., Dressler, G., Mayer, N., and Johnson, L., "Development and Flight Qualification of the Propulsion and Reaction Control System for ERIS," AIAA Paper 92-3663, July 1992.

[13]Chazen, M., Calvignac, J., and Sicher, D., "G02-C2H5OH Workhorse Engine," AIAA Paper 98-3819, July 1998.

[14]Mueller, T., and Dressler, G., "TRW 40 KLBf LOX/RP 1 Low Cost Pintle Engine Test Results," AIAA Paper 2000-3863, July 2000.

[15]Gavitt, K., and Mueller, T., "Testing of the 650 Klbf LOX/LH2 Low Cost Pintle Engine (LCPE)," AIAA Paper 2001-3987, July 2001.

[16]Anderson, W. A., and Meyer, S. E., "Propulsion Test Facilities at Purdue University," AIAA Paper 2002-4028, 2002.

[17]Austin, B. L., Matthews, J. B., and Heister, S. D., "Engine/Injector Development for New Nontoxic Storable Bipropellants," *13th Annual Propulsion Engineering Research Symposium*, Oct. 2001.

[18]Cahill, D. M., et al., "Assessment of Wind Tunnel Data Uncertainty," AIAA Standard Publication AIAA S-071-1995, 1995.

[19]Austin, B. L., "Characterization of Pintle Engine Performance for Nontoxic Hypergolic Bipropellants," M.S. Thesis, School of Aeronautics and Astronautics, Purdue Univ., West Lafayette, IN, 2002.